文章编号：0258-7106（2019）05-1147-12 Doi: 10. 16111/j. 0258-7106. 2019. 05. 013

湘南圳口石英脉型黑钨矿床白云母 Ar-Ar 同位素测年及其对区域找矿勘查的指示

严 宸[1,2]，赵海杰[1**]，赵盼捞[1]，袁顺达[1]

（1 中国地质科学院矿产资源研究所 自然资源部成矿作用与矿产资源评价重点实验室，北京 100037；
2 中国地质大学，北京 100083）

摘 要 彭公庙岩体是南岭地区早古生代大花岗岩基的典型代表之一，在其周围发育有圳口、张家垄及杨梅坑等大-中型的钨矿床（点）。由于钨矿化主要产出于彭公庙岩体的内部及其周缘地层中，这些矿床过去一直被认为形成于早古生代，与彭公庙岩体有着紧密的成因联系。然而，这些矿床与大花岗岩基的时间及成因关系尚未准确厘定。文章在已有研究的基础上，对圳口钨矿进行了高精度白云母 Ar-Ar 测年，获得坪年龄为（148.0±0.7）Ma（MSDW=3.1），对应的等时线年龄为（148.1±0.8）Ma（MSDW=2.6），反等时线年龄为（148.1±0.8）Ma（MSDW=2.6），表明圳口钨矿床形成于晚侏罗世，明显晚于早古生代彭公庙大花岗岩基的侵位时间，是南岭地区中-晚侏罗世大规模钨锡成矿事件的一部分。通过总结研究发现，区域上早古生代花岗岩基周缘的钨锡矿床均形成于晚侏罗世，该结论不仅表明研究区深部晚侏罗世岩浆活动强烈，而且指示区内不同矿床之间在成因上密切相关。整个区域上的矿床类型和空间分布显示出不同的围岩性质制约了不同的矿化过程，从而形成不同的矿床类型。含矿热液沿着裂隙通道向上运移，当围岩为花岗岩时，形成了石英脉-云英岩型矿床，而当围岩为碎屑岩时，则形成石英脉型矿床。这些不同类型矿床可以构成一套矿床组合模型，互为找矿指示。

关键词 地球化学；Ar-Ar 测年；早古生代；彭公庙岩体；圳口钨矿；湘南

中图分类号：P618.67 **文献标志码**：A

Muscovite Ar-Ar isotopic dating of Zhenkou quartz vein type wolframite deposit in southern Hunan Province and its significance for regional exploration

YAN Chen[1,2], ZHAO HaiJie[1], ZHAO PanLao[1] and YUAN ShunDa[1]

(1 MNR Key Laboratory of Metallogeny and Mineral Assessment, Institute of Mineral Resources, Chinese Academy of Geological Sciences, Beijing 100037,China; 2 China University of Geosciences, Beijing 100083, China)

Abstract

The Penggongmiao granite batholith is one of the typical representatives of the Early Palaeozoic large granite batholiths in the Nanling region. Recently, large to medium-sized tungsten deposits, such as Zhenkou, Zhangjialong and Yangmeikeng, were discovered around the Penggongmiao granite batholith. Because of the main orebodies present in the interior of the Penggongmiao granite batholith and the surrounding strata, these deposits are considered that formation of Early Palaeozoic and relate to Penggongmiao granite. However, the timing and genetic relationship between these deposits and large granite batholith is unclear. Based on the existed research, the high-precision muscovite Ar-Ar dating of the Zhenkou tungsten deposit was carried out, and yielded a well-defined $^{40}Ar/^{39}Ar$

* 本文得到国家自然科学基金项目（编号：41672095、41773041）、优秀青年科学基金项目（编号：41822304）和中国地质科学院基本科研业务费专项经费（编号：YYWF201711）联合资助

第一作者简介 严 宸，男，1994 年生，硕士，矿物学、岩石学、矿床学专业。Email: 649861224@qq.com

* * 通讯作者 赵海杰，女，1982 年生，副研究员，矿物学、岩石学、矿床学专业。Email: zhaohaijie_610@163.com

收稿日期 2019-04-01；改回日期 2019-05-13。秦思婷编辑。

plateau age of (148.0±0.7) Ma(MSDW=3.1), with an isochron age of (148.1±0.8) Ma（MSDW=2.6）and an inverse isochron age of (148.1±0.8) Ma（MSDW=2.6）, indicating that the Zhenkou tungsten deposit formed in the Late Jurassic. This age is consistent with the Zhenkou tungsten deposit was formed in the Late Jurassic and obviously later than the emplacement time of the Early Palaeozoic Penggongmiao granite batholith, which is part of the large-scale tungsten-tin metallogenic event of the Late Jurassic in the Nanling region. The comparative study on the area shows that the tungsten and tin deposits around the periphery of the Early Palaeozoic granite in the region are formed in the Late Jurassic, indicating not only the intense Late Jurassic granite magmatic activity of the deep, but also the close genetic relationship between different deposits in the area. The deposit types and spatial distribution in the whole region show that different physicochemical properties of wall rock may control the mineralization processes and ore deposit types. The ore-bearing hydrothermal fluid was brought by granite emplacement, and migrated along the presence of fault channe lways. When the surrounding rock is granite, quartz vein - greisen type deposit is formed, and when the surrounding rock is Sinian clastic rock, quartz vein type deposit may be formed. Therefore, different types of deposits can forming metallogenic model, which are prospecting indicators for each other.

Key words: geochemistry, Ar-Ar dating, Early Palaeozoic, Penggongmiao granite, Zhenkou tungsten, southern Hunan Province

研究表明，原生钨锡矿床在时、空及成因上多与花岗岩密切相关，花岗质岩浆通常被认为是钨锡矿床成矿元素的主要来源(Ferguson et al., 1912; Taylor, 1979; Kwak, 1987; Heinrich, 1990; Lehmann, 1990; Štemprok, 1995)。南岭是世界上最重要的钨锡多金属成矿带，区内一系列超大型、大-中型钨锡多金属矿床与广泛分布的花岗岩有密切的成因联系。南岭地区的构造演化复杂，先后经历了加里东期、印支期以及燕山期构造运动。多期构造-岩浆事件，复杂的岩浆活动以及后期热液作用往往在同一岩体或矿床内部相互叠加，导致不同期次的花岗质岩体侵位和多期的成矿作用在一个矿区叠加，使研究矿床成因及进一步找矿勘查工作的部署都遇到了挑战。长期以来，区内一系列与多期岩浆活动有关的钨锡矿床，由于矿床年龄缺乏精确的年代学数据约束，导致不同学者对其形成时代和成因机制的认识往往存在着较大分歧，典型的矿床如荷花坪锡矿、锡田锡矿、邓阜仙锡矿、云头界钨矿（图1）（蔡杨等，2012；伍静等，2012；郭春丽等，2014；Zhang et al., 2015）。因此，精确的矿床年龄对厘定复式岩体与相关钨锡矿床成岩成矿的时空关系，对理解这一类型矿床的形成机制，以及区域找矿勘查部署都有着重要的意义。

南岭地区早古生代大花岗岩基出露面积仅次于中生代花岗岩（Yuan S D et al., 2018）。近年来，苗儿山-越城岭和彭公庙-桂东等早古生代大花岗岩基周围一系列钨锡矿床（点）的发现（图1），显示同期大花岗岩基及其周缘具有寻找钨锡矿的重大潜力，因此，南岭早古生代钨锡成矿作用也逐渐受到关注（张文兰等，2011；李时谦等，2013；华仁民等，2013；陈骏等，2013）。张文兰等（2011）通过锆石 LA-ICP-MS U-Pb 测年表明彭公庙岩体中粗粒似斑状黑云母花岗岩和张家垄坑道内的含白钨矿细晶岩脉分别形成于(436.2±3.1)Ma 和(426.5±2.5)Ma。基于这些年代学数据，彭公庙地区的钨矿床被认为是早古生代大花岗岩基成矿的典型代表（乔玉生等，2011；李时谦等，2013）。然而，细晶岩脉与钨矿化之间的时、空及成因关系并不明确。为进一步明确区内矿床与彭公庙大花岗岩基的联系，本文在已有研究的基础上，对圳口钨矿床中与黑钨矿共生的白云母开展了高精度的 ^{39}Ar-^{40}Ar 测年，为深入研究区域成岩成矿时空架构提供年代学依据。

1 区域地质

南岭位于华南腹地，构造上处于华夏板块西北缘，总面积约 170 000 km^2（图1）。基底主要由震旦系—志留系的浅变质岩组成，盖层则由泥盆系—三叠系的碳酸盐岩和碎屑岩组成。该区经过加里东期、印支期、燕山期多期构造事件，基底发生强烈的褶皱和变形，区内裂谷盆地广泛分布（舒良树等，2006）。

在多旋回构造岩浆活动背景下，不同时代的花岗岩广泛发育，并伴有巨量的钨、锡和稀有金属等矿

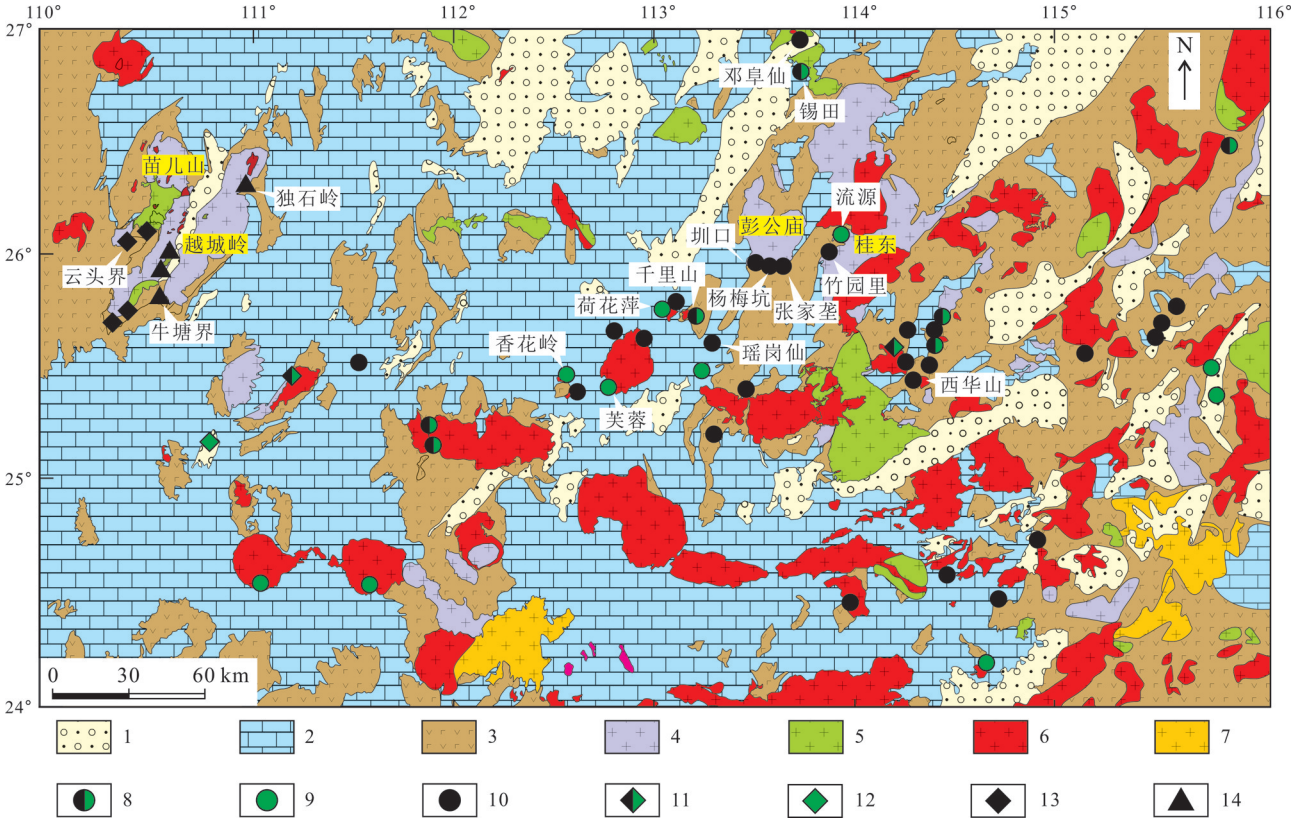

图 1 南岭地区花岗岩以及主要钨锡矿床分布图(据毛景文等,2008;Zhao et al., 2018 修改)

1—侏罗系—白垩系碎屑岩、火山岩和红层;2—泥盆系—三叠系碳酸盐岩;3—前志留系碎屑岩;4—加里东期花岗岩;5—印支期花岗岩;6—燕山期花岗岩;7—晚燕山期花岗岩;8—燕山期钨锡矿床;9—燕山期锡矿床;10—燕山期钨矿床;11—印支期钨锡矿床;12—印支期锡矿床;13—印支期钨矿床;14—加里东期钨矿床

Fig.1 Geologic map of the Nanling Range showing the distribution of granites and associated tungsten/tin deposits (modified after Mao et al., 2008; Zhao et al., 2018)

1—Jurassic—Cretaceous clastic and volcanic rocks and redbeds; 2—Devonian to Triassic carbonate; 3—Pre-Silurian clastic rocks; 4—Caledonian granite; 5—Indosinian granite; 6—Yanshanian granite; 7—Late Yanshan granite; 8—Yanshanian W-Sn deposit; 9—Yanshanian Sn deposit; 10—Yanshanian W deposits; 11—Indosinian W-Sn deposit; 12—Indosinian Sn deposit; 13—Indosinian W deposit; 13—Caledonian tungsten deposit

床的形成。晚侏罗世是南岭巨量钨锡多金属富集成矿的重要时期,由于太平洋板块的俯冲以及大陆地壳的不断加厚,在弧后伸展带发育一条 NE 向的花岗岩带,并伴随大规模钨锡成矿作用(毛景文等,2008; Zhao et al., 2017),形成了西华山、大吉山、瑶岗仙、柿竹园、香花岭及芙蓉等一系列超大型、大型钨锡矿床。高精度的年代学数据显示,该期大规模钨锡成矿事件主要集中于 160~150 Ma(刘晓菲等,2012;Yuan et al., 2007;2008;2011; Hu et al., 2012a, 2012b; 原垭斌等,2014;赵盼捞等,2016)。与燕山期强烈构造-岩浆作用类似,南岭地区于加里东期亦经历了强烈的构造-岩浆作用,不仅导致大规模前泥盆系基底的强烈变质变形及广泛的区域不整合,而且发育大规模花岗质岩浆岩侵位(舒良树等,2006;Wang et al., 2007)。区内的加里东期(早古生代)花岗岩大多具有 S 型花岗岩的特征,空间上主要分布于华夏地块及其与扬子地块的交界地区,呈大岩基产出(孙涛,2006;伍光英等,2008;华仁民等,2013)。这些大花岗岩基形成后,往往经历印支期及燕山期的构造-岩浆活动的叠加改造,形成复式花岗岩体,并伴有多期次的钨锡多金属成矿作用(Mao et al., 2013; 袁顺达,2017)。苗儿山-越城岭和彭公庙-桂东被认为是南岭地区加里东期大岩基成矿的典型代表。然而,苗儿山-越城岭大岩基周围的钨锡矿床不仅有独石岭、牛塘界等加里东期钨锡矿床(杨振等,2014;陈文迪等,2016),还存在油

麻岭、高岭、云头界等印支期钨锡矿床(伍静等,2012;杨振等,2013;张迪等,2015),而彭公庙-桂东大岩基周围的张家垄、竹园里和流源等钨锡矿床近期已有年代学数据表明其为燕山期矿床(Yuan S D et al., 2018; Yuan Y B et al., 2018)。

2 矿床地质

圳口钨矿位于彭公庙大岩基的南缘,是一个以石英脉型黑钨矿为主的中型钨矿床。矿体主要产出于震旦系下统正园岭组中(图3)。震旦系下统正园岭组是矿区内唯一出露的地层,也是主要的赋矿围岩,主体岩性为灰色-灰绿色中厚层状浅变质石英砂岩、长石石英砂岩,夹有少量灰绿色薄层状板岩。区内断裂构造发育,可分为EW向、NW向和NNE向3组(图2)。其中,EW向断裂为区域性构造,控制彭公庙大花岗岩基的侵位,而NW向断裂为矿区主要的控矿容矿构造,其形成时代晚于EW向断裂,穿切了彭公庙大岩基,并且NW向断裂也是矿区内数量最多、分布最密集的断裂构造;而NNE向断裂为成矿后断裂,形成时代最晚,不仅穿切了彭公庙大岩基还穿切了NW向断裂以及NW向断裂中的矿体。彭公庙地区的出露的岩浆岩主要为加里东期(早古生代)的彭公庙大花岗岩基,出露面积达970 km^2(Yuan S D et al., 2018),基于其岩相学及年代学证据,该大花岗岩基又可被划分为早、晚两期(图2;Zhang et al., 2014)早期花岗岩为细粒似斑状黑云母二长花岗岩,出露面积约占彭公庙大岩基的25%,分布于大岩

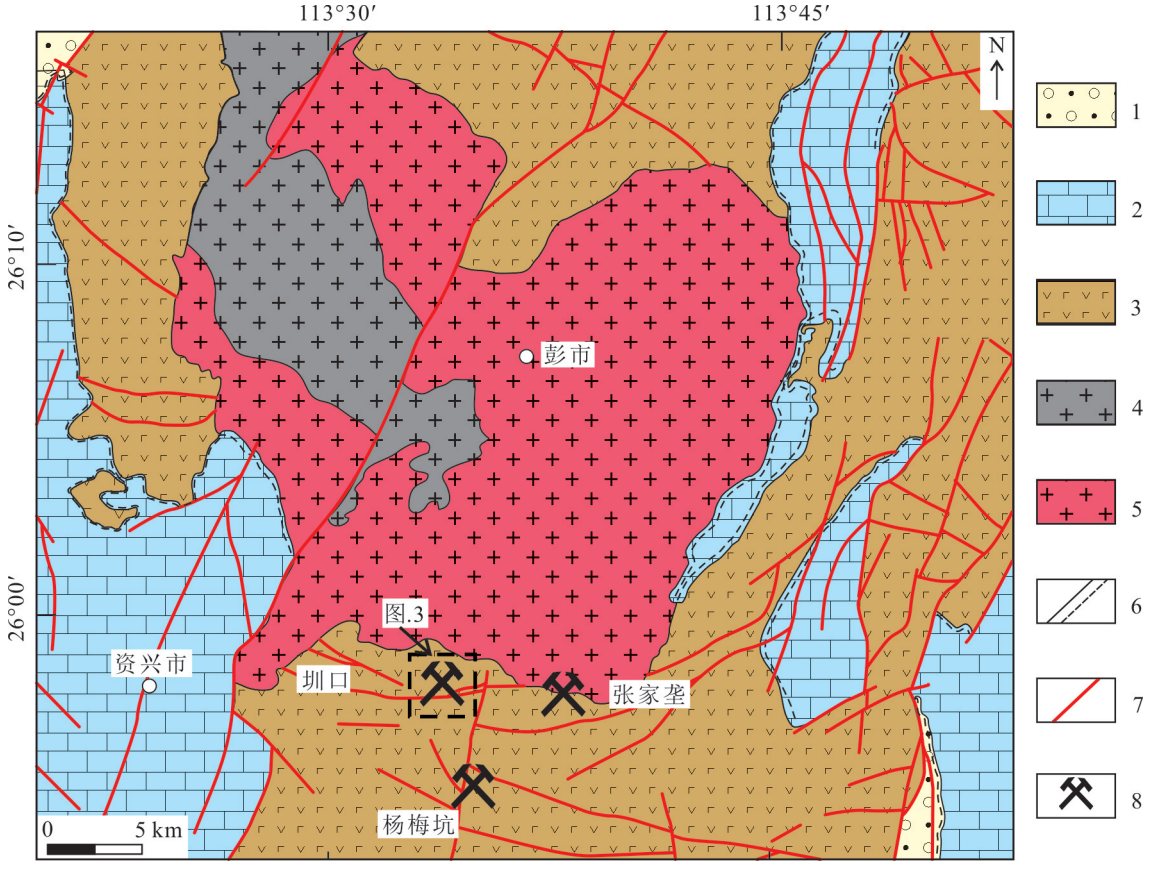

图2 彭公庙地区地质图(据李时谦等,2013修改)

1—侏罗系—白垩系砂岩和砾岩;2—泥盆系—三叠系灰岩、页岩和砂岩;3—前奥陶系变质砂岩;4—加里东期细粒似斑状黑云母二长花岗岩(早);5—加里东期中、粗粒似斑状黑云母二长花岗岩(晚);6—不整合面;7—断层;8—钨矿床

Fig.2 Geologic sketch map of the Penggongmiao area (modified after Li et al., 2013)

1—Jurassic—Cretaceous sandstone and conglomerate; 2—Devonian to Triassic limestone, shale and sandstone; 3—Pre-Ordovician metasandstone; 4—Caledonian fine-grained porphyroid biotite monzogranite (Early); 5—Caledonian fine-grained porphyroid biotite monzogranite (Late); 6—Unconformity; 7—Fault; 8—W deposit

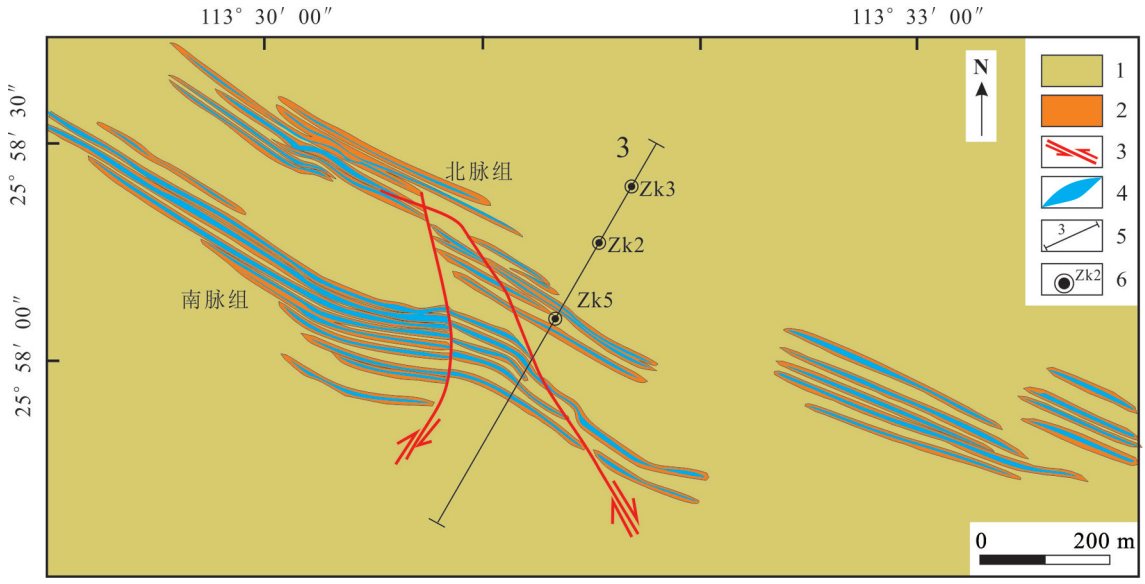

图3 圳口钨矿矿区地质图(据湖南省资兴县圳口钨铋矿区详细普查报告,1966 修改)

1—震旦系下统正圆岭组石英砂岩;2—蚀变带;3—断层;4—钨矿脉;5—勘探线及其编号;6—钻孔及其编号

Fig.3 Geologic sketch map of the Zhenkou tungsten deposit (modified after Detailed Survey Report on Shenkou Tungsten Bismuth Mining Area, Zixing County, Hunan Province, 1996)

1—Lower Sinian Zhengyuanling Formation quartz sandstone; 2—Alteration zone; 3—Fault; 4—Tungsten vein; 5—Exploration line and its number; 6—Drill hole and its number

基的中心以及西北部,锆石 LA-ICP-MS U-Pb 年龄为 447~442 Ma;晚期花岗岩为中-粗粒似斑状黑云母二长花岗岩,占岩体面积 70% 以上,主要分布于大岩基的边部,锆石 LA-ICP-MS U-Pb 年龄为 436~431 Ma。彭公庙花岗岩整体呈灰白色,似斑状结构,斑晶主要为微斜长石和斜长石,基质主要由钾长石、斜长石、石英和黑云母组成。

圳口钨矿区面积约 0.5 km^2,近东西向展布长约 2000 m,宽约 250 m。矿体共由 100 多条 NW 走向含矿石英脉组成,根据脉体形状可分为石英大脉带型和石英细脉带型;根据空间分布特征可为南、北 2 个部分,二者近状平行产出(图 3)。其中,北脉组长 1200 m,宽 50~60 m,共有大小石英脉 25 条,总脉厚 1.6~3.2 m,控制斜深 600 m;南脉组长 1360 m,宽 110~250 m,共有大小石英脉 95 条,总脉厚 2~7 m,控制斜深 500 m。根据矿石的结构构造和矿物组合将矿化阶段可分为,氧化物阶段、硫化物阶段和碳酸盐阶段。其中,氧化物阶段是圳口钨矿的主要成矿阶段,以石英、黑钨矿为主。脉体可见明显的分带,边部为白云母、黑钨矿,往里为绿柱石、黄玉,中心为石英和少量白钨矿。硫化物阶段以石英、辉铋矿和黄铁矿为主,同时白钨矿在该阶段普遍存在,但矿化程度较弱,并可见部分白钨矿交代早期形成的黑钨矿。碳酸盐阶段则以方解石为主,并有少量的绿泥石化。矿石主要呈他形-半自形-自形晶结构、交代结构、乳滴状及压碎结构等;矿石构造主要有浸染状、条带状、细脉状、团块状及放射状构造。矿石矿物主要为黑钨矿和辉锑矿,并发育有白钨矿、辉钼矿、黄铁矿和少量黄铜矿、铁闪锌矿;脉石矿物主要为石英、白云母和萤石(李时谦等,2013;郭爱民,2011)。矿区内的热液蚀变和矿化主要受到断裂控制,沿着断裂两侧分布(图 2),主要的蚀变类型包括硅化、黄铁矿化、绿泥石化、云英岩化、绢云母化、绿帘石化以及碳酸盐化。其中,硅化和黄铁矿化与成矿关系最为密切。

3 样品采集与分析

本次用于 Ar-Ar 测年的样品(ZK-6)采自于圳口矿区石英脉型黑钨矿石。矿石矿物主要由石英、黑钨矿及白云母组成(图 4a、b),白云母主要分布于石英脉的脉体边缘(图 4a),与石英和黑钨矿密切共生,

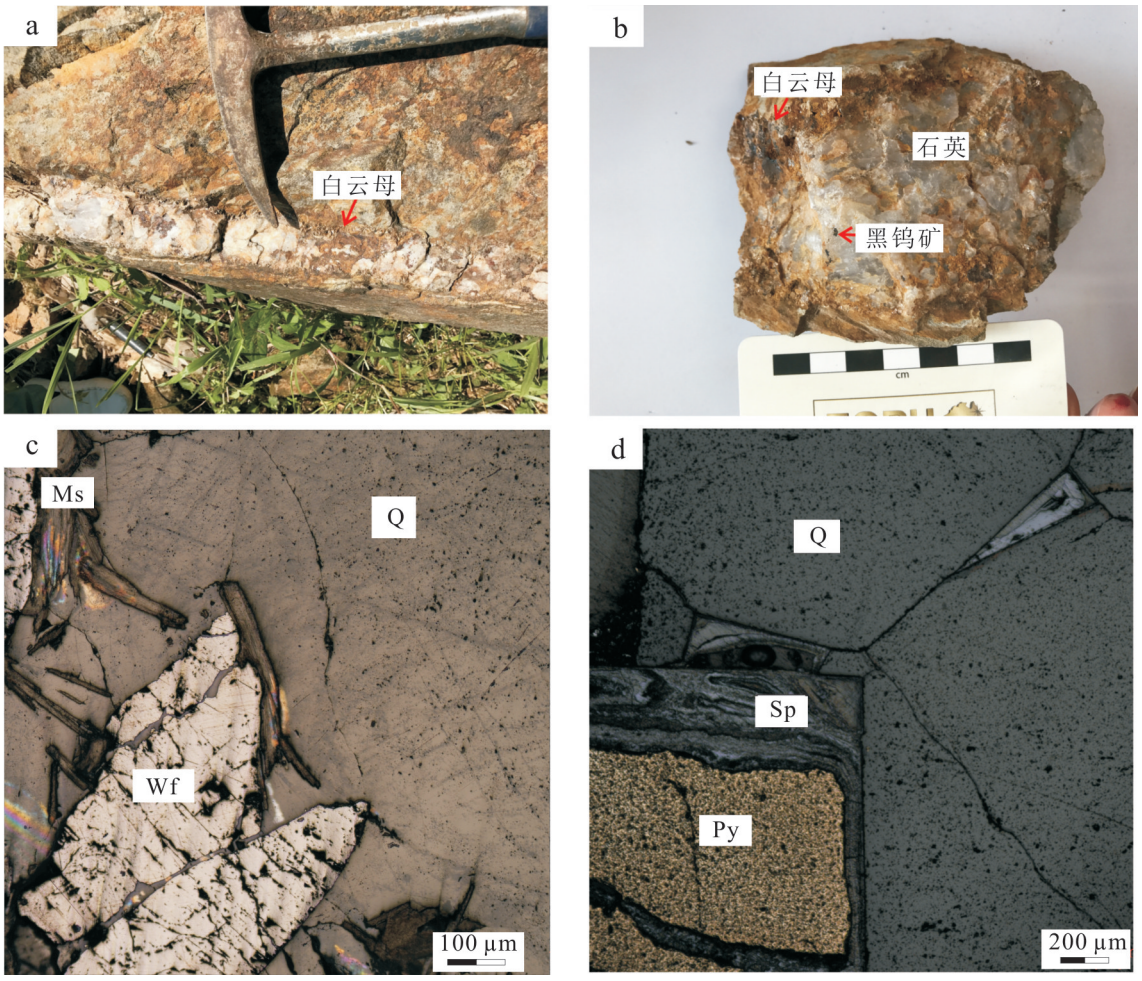

图4 圳口石英脉型黑钨矿矿石野外、手标本和镜下照片

a. 含矿石英脉野外照片;b. 石英脉型黑钨矿矿石手标本照片;c. 石英(Q)脉中的黑钨矿(Wf)和白云母(Ms)(反射光);d. 石英脉中黄铁矿(Py)和闪锌矿(Sp)(反射光)

Fig.4 Photographs of hand specimens, and microphotographs of ore-hosted quartz vein from Zhenkou tungsten deposit

a. Ore-bearing quartz veins; b. Photographs of hand specimens of quartz vein type wolframite ore; c. Wolframite (Wf) and muscovite (Ms) in quartz (Q) veins (under reflected light); d. Pyrite (Py) and sphalerite (Sp) in quartz veins (under reflected light)

显微镜下可见石英颗粒间发育黄铁矿和闪锌矿(图4d)。在野外和室内观察的基础上选取与成矿相关的白云母样品,经过破碎、筛选至60~80目,在双目镜下挑选使选取的白云母的纯度达到99%,用超声波清洗。清洗后的样品被封装进石英瓶送核反应堆中接收照射。照射工作是在中国原子能科学研究院的"游泳池堆"中进行的,使用B4孔道,中子流密度约为2.65×10^{13} n $cm^{-2}S^{-1}$。照射总时间为1440 min,积分中子通量为2.29×10^{18} n cm^{-2};同期接受中子照射的还有用做监控样的标准样:ZBH-25黑云母标样,其标准年龄为(132.7±1.2)Ma,w(K)为7.6%。

样品的阶段升温加热使用石墨炉,每一个阶段加热10 min,净化20 min。质谱分析是在中国地质科学院地质研究所Ar-Ar年代学同位素实验室用多接收稀有气体质谱仪Helix MC上进行的,每个峰值均采集20组数据。所有的数据在回归到时间零点值后再进行质量歧视校正、大气氩校正、空白校正和干扰元素同位素校正。中子照射过程中所产生的干扰同位素校正系数通过分析照射过的K_2SO_4和CaF_2来获得,其值为:$(^{36}Ar/^{37}Ar_o)_{Ca}$=0.000 2398,$(^{40}Ar/^{39}Ar)_K$=0.004 782;$(^{39}Ar/^{37}Ar_o)_{Ca}$=0.000 806。^{37}Ar经过放射性衰变校正;^{40}K衰变常数$\lambda=5.543\times10^{-10}a^{-1}$;用ArArCALC程序计算坪年龄及正、反等时线(Anthony Koppers,v2.5.2,2012)。坪年

龄误差以2σ给出。详细实验流程见有关文章(陈文等,2006;张彦等,2006)。

4 测试结果

圳口石英脉型黑钨矿中白云母(ZK-6)的阶段加热^{40}Ar-^{39}Ar同位素分析结果列于表1,相应的表观年龄谱、等时线年龄及反等时线年龄如图5 a、b所示。在800~1400℃温度范围内对样品进行了11个阶段的释热分析。从表1可以看出,样品在低温释热阶段的视年龄较小,这可能是由于矿物低温晶格缺陷或矿物表面少量Ar丢失所致(Hanson et al., 1975;邱华宁等,1997;袁顺达等,2012),而在高温释热阶段构成了很好的年龄坪。样品总气体年龄为152.6 Ma,在高温释热阶段(960~1190℃)构成的坪年龄为(148.0±0.7) Ma(图5a),对应了95.25%的^{39}Ar释放量,相应的^{36}Ar/^{40}Ar-^{39}Ar/^{40}Ar反等时线年龄为(148.1±0.8) Ma(MSWD=2.1),^{40}Ar/^{36}Ar初始值为(290.9±3.2)(图5b)。从分析结果可以看出,样品的总气体年龄、坪年龄、相应的等时线年龄和反等时线年龄在误差范围内完全一致,因而样品的坪年龄(148.0±0.7 Ma)可以代表白云母的结晶年龄。

5 讨 论

5.1 成岩成矿时代

彭公庙大花岗岩基主要由早期的细粒似斑状黑云母花岗岩和晚期中-粗粒似斑状黑云母花岗岩组成(图2),对应的锆石U-Pb年龄为447~431 Ma,表明彭公庙大花岗岩基形成于早古生代(Zhang et al., 2014)。大花岗岩基的南缘发育有强烈的钨矿化,矿化主要集中于岩体内部以及周围地层中,紧密的空

表1 圳口钨矿白云母 ^{40}Ar/^{39}Ar 阶段升温测年数据

Table 1 ^{40}Ar/^{39}Ar stepwise heating analytical data for muscovite from the Zhenkou tungsten deposit

温度/℃	$(^{40}Ar/^{39}Ar)_m$	$(^{37}Ar/^{39}Ar)_m$	$(^{36}Ar/^{39}Ar)_m$	$^{40}Ar^*/^{39}Ar_k$	±1σ	年龄/Ma	误差/Ma
800	1093.02367	0	3.67532	6.96242	7.03	48.03	47.88
860	78.65981	0	0.19856	19.98164	0.38	134.57	2.47
920	510.09224	0	1.70091	7.46762	3.23	51.47	21.98
960	35.27480	0	0.04521	21.91002	0.09	147.04	0.60
1000	23.69092	0	0.00554	22.04937	0.04	147.94	0.24
1040	22.73779	0	0.00244	22.01294	0.04	147.70	0.24
1070	22.63412	0	0.00179	22.09919	0.04	148.26	0.24
1100	26.88012	0	0.01689	21.88309	0.05	146.87	0.35
1140	24.10452	0	0.00658	22.15625	0.06	148.63	0.36
1190	27.72790	0	0.01894	22.12655	0.11	148.43	0.70
1400	60.43575	0	0.14390	17.90841	0.41	121.06	2.69

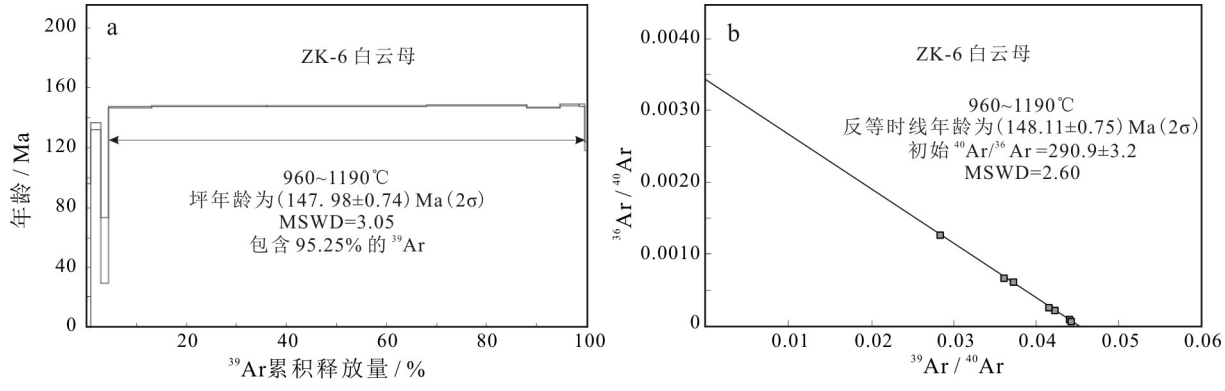

图5 圳口钨矿床白云母Ar-Ar坪年龄(a)和反等时线年龄(b)

Fig.5 ^{40}Ar-^{39}Ar age spectrum(a) and inverse isochron(b) of muscovite from the Zhenkou tungsten deposit

间关系使得圳口、张家垄和杨梅坑等钨矿床(点)一度被认为与彭公庙大花岗岩基有关,是早古生代成矿的典型代表(乔玉生等,2011;李时谦等,2013)。张文兰等(2011)于张家垄钨矿区获得白钨矿化细晶岩的锆石U-Pb年龄为(426.5±2.5)Ma,该年龄稍晚于大花岗岩基的成岩年龄,认为细晶岩可能是彭公庙大花岗岩基演化至晚期的产物。细晶岩中的白钨矿化也被认为是彭公庙大花岗岩基高度分异演化晚期残余熔体中高度富集成矿元素钨、锡的表现。但是,细晶岩和矿体的空间关系未知,且细晶岩中白钨矿与矿化之间的成因联系也不明确,所以,细晶岩的锆石U-Pb年龄能否直接代表矿床的形成年龄?仍存在疑问。

矿石中含钾蚀变矿物的Ar-Ar年龄是厘定矿床成矿时代的有效手段之一,已经被广泛应用于各类热液矿床成矿年代学研究(Peng et al., 2006;彭建堂等,2007;Yuan et al., 2007;袁顺达等,2012)。圳口含黑钨矿石英脉中,白云母与黑钨矿密切共生(图4c),因此,白云母的Ar-Ar年龄能够代表石英脉型黑钨矿床的形成年龄。本次研究获得的白云母Ar-Ar坪年龄为(148.0±0.7)Ma,该年龄直接指示了圳口钨矿床形成于晚侏罗世,而与之前认为的早古生代成矿存在明显的时差。

5.2 矿床成因

圳口钨矿与张家垄钨矿是彭公庙岩体周围2个主要的钨矿床(点)。其中,张家垄钨矿以云英岩和石英脉型白钨矿为主,矿体产出于彭公庙岩体内部,围岩主要为早古生代的中-粗粒似斑状黑云母二长花岗岩(图2),围岩蚀变主要受到断裂控制,蚀变类型以云英岩化、硅化、绢云母化和绿泥石化为主,其中云英岩化和硅化与成矿关系密切(乔玉生等,2011)。圳口钨矿以石英脉型黑钨矿为主,矿体主要产出于震旦系下统正园岭组砂岩中。上述2个矿床虽然产出位置不同,在空间上都与彭公庙大花岗岩基有明显联系,但在大花岗岩基内部却没有发现典型的从碱交代-云英岩化-硅化的热液蚀变分带,反而区域上的钨矿化以及热液蚀变明显受到了NW向和NWW向断裂带的控制(图3)。这与野外观察到矿化蚀变沿脉体两侧发育,蚀变强度与离脉体距离成反比,距离脉体越远,矿化蚀变越弱,远端几乎无蚀变的现象一致,暗示了成矿流体来自于后期热液活动。此外本次获得圳口钨矿的白云母Ar-Ar坪年龄(148.0±0.7) Ma,与Yuan S D等(2018)获得的张家垄钨矿床的辉钼矿Re-Os (160.4±2.2) Ma以及白云母Ar-Ar (153.5±1.0) Ma相近,表明了彭公庙岩体附近的钨矿床形成于晚侏罗世。因此,彭公庙地区的钨矿化与早古生代的大花岗岩基缺乏直接的成因联系,而可能与彭公庙大岩基深部隐伏的晚侏罗世花岗岩有关。

与彭公庙大花岗岩基相邻的早古生代桂东大花岗岩基(图1),其西南缘发育有竹园里钨矿和流源锡矿,矿化以云英岩型和石英脉型为主。矿体主要产于桂东大花岗岩基内部,围岩主要为早古生代的中-粗粒黑云母花岗岩,蚀变类型有云英岩化、绿泥石化和硅化,其中云英岩化与钨锡矿化关系密切。矿化蚀变特征与圳口钨矿和张家垄钨矿相似,明显受到了区域上断裂的控制,云英岩化沿着断裂两侧分布,随着离断裂中心距离的增加,矿化蚀变逐渐消失(Yuan Y B et al., 2018)。竹园里钨矿和流源锡矿之前也被认为是形成于早古生代的钨锡矿床(易元顺等,2014),然而,竹园里钨矿的白云母Ar-Ar坪年龄为(151.6 ± 1.0) Ma,流源锡矿的白云母Ar-Ar坪年龄为(153.1±1.0) Ma(Yuan Y B et al., 2018),显示了竹园里钨矿和流源锡矿的形成也与桂东大花岗岩基深部隐伏的晚侏罗世花岗岩有关。综上所述,彭公庙-桂东地区大岩基周围的圳口钨矿、张家垄钨矿、竹园里钨矿和流源锡矿的形成均与晚侏罗世花岗岩的侵位活动密不可分。区内矿床年龄在160~147 Ma之间,时间上与南岭地区中-晚侏罗世大规模钨锡成矿吻合(彭建堂等,2008;刘晓菲等,2012;赵盼捞等,2016),因而彭公庙-桂东大岩基周围的钨锡矿化与区域上的大规模钨锡成矿事件是同一构造岩浆活动的产物。

5.3 区域矿床组合

南岭是世界上最大的钨锡多金属成矿带,大量的年代学数据表明,钨锡矿床的形成时代主要集中于晚侏罗世(160~150Ma)和晚白垩世(90~70 Ma),部分为晚三叠世(240~220 Ma,Hu et al., 2012; Mao et al., 2013),这些钨锡矿床空间分布和成因多与高分异的小岩体有关。

早古生代花岗岩在区域上分布广泛,但多呈大岩基出露地表,而在南岭地区大面积出露的花岗岩基由于分异演化程度较低基本不能直接形成钨锡矿床(Lehmann, 1982;袁顺达, 2017;Yuan S D et al., 2018)。

彭公庙-桂东大岩基周围的圳口、张家垄、竹园

里钨矿和流源锡矿床均产出于大岩基内部或周缘地层中(图1),一直被认为是早古生代花岗岩成矿的代表,但地质特征和年代学研究数据显示这些矿床均形成于晚侏罗世,因此,区内钨锡矿床的形成可能与深部燕山期的构造岩浆活动有关。晚侏罗世花岗岩的侵位带来的含矿热液在温度和压力梯度的作用下,沿着早期花岗岩(围岩)中存在的裂隙通道上升,上升的过程中含矿热液不断的渗透交代裂隙两侧的围岩,最终因所处物理化学条件的改变导致钨锡矿的沉淀(Wood et al., 2000)。钨锡矿的类型和矿床组合特点主要受到了围岩性质及构造条件的控制,不同的围岩性质和构造条件制约了不同的矿化过程,从而形成不同的矿床组合(Dewaele et al., 2016; Hulsbosch et al., 2016)。彭公庙-桂东地区围岩性质的差异,制约了钨锡矿床的类型。当围岩为花岗岩时,强烈的水岩反应使得断裂两侧的花岗岩发生云英岩化(Burt, 1981),形成了以云英岩为主的云英岩-石英脉型的钨锡矿床组合,如张家垄云英岩型白钨矿矿床、竹园里云英岩型白钨矿矿床和流源石英脉型锡矿床;而当围岩为碎屑岩时,沿构造通道(断裂带)或层间薄弱面发育石英脉型-层控型钨锡矿床组合,如圳口石英脉型黑钨矿矿床和杨梅坑层控型白钨矿矿床。这些矿床都是相同构造岩浆事件的产物,同一系统中不同类型矿床可以互为找矿标志。

6 结 论

(1)圳口钨矿床与黑钨矿共生的白云母^{39}Ar-^{40}Ar坪年龄为(148.0 ± 0.7) Ma,指示了圳口钨矿形成于晚侏罗世,与彭公庙大花岗岩基深部隐伏的晚侏罗世花岗岩有关。

(2)野外地质观察表明,彭公庙-桂东岩体内部缺乏典型的矿化蚀变分带,且钨锡矿化明显受到的断裂的控制,矿化蚀变沿着断裂两侧分布。圳口、张家垄、流源和竹园里钨锡矿床年代学数据显示彭公庙-桂东地区的钨锡矿化均发生在160~147 Ma之间,与南岭中-晚侏罗世大规模钨锡成矿是同一构造岩浆事件的产物。

(3)围岩的差异导致了矿化类型的不同,当围岩为花岗岩时,形成了云英岩-石英脉型白钨矿(锡)矿床,而当围岩为震旦系碎屑岩时,则形成了石英脉型黑钨矿矿床。

致 谢 野外样品采集工作中的得到了湘南地质勘查原张怡军工程师的帮助;Ar-Ar测试以及数据处理过程中得到了中国地质科学院张彦副研究员的帮助;资料收集和论文的撰写过程中得到了中国地质科学院原垭斌和陶旭云的帮助;匿名审稿专家为文章修改提出许多建设性意见,在此一并表示感谢!

References

Burt D M. 1981. Acidity-salinity diagrams application to greisen and porphyry deposits[J]. Econ. Geol., 76(4):832-843.

Chen W, Zhang Y, Jing G S and Zhang Y Q. 2006. Late Cenozoic episodic uplifting in southeastern part of the Tibetan Pateau-evidence from Ar-Ar thermochronology[J]. Acta Petrologica Sinica, 22(4): 867-872(in Chinese with English abstract).

Chen W D, Zhang W L, Wang R C, Chu Z Y, Xiao R, Zhang D and Che X D. 2016. A study on the Dushiling tungsten-copper deposit in the Miao'ershan-Yuechengling area, northern Guangxi, China: Implications for variations in the mineralization of multi-aged composite granite plutons[J]. Science China Earth Sciences, 59 (11): 2121-2141(in Chinese with English abstract).

Cai Y, Ma D S, Lu J J, Huang H, Zhang R Q and Qu W J. 2012. Re-Os geochronology and S isotope geochemistry of Dengfuxian tungsten deposit, Hunan Province, China[J]. Acta Petrologica Sinica, 28(12):3798-3808(in Chinese with English abstract).

Dewaele S, De Clercq F, Hulsbosch N, Piessens K, Boyce A, Burgess R and Muchez P. 2016. Genesis of the vein-type tungsten mineralization at Nyakabingo (Rwanda) in the Karagwe-Ankole belt, Central Africa[J]. Mineralium Deposita, 51(2): 283-307.

Ferguson H G and Bateman A M. 1912. Geologic features of tin deposits[J]. Econ. Geol., 7(3): 209-262.

Guo A M. 2011. Geological characteristics and prospecting potential of Zhangjialong tungsten deposit in Zixing, Hunan Province[J]. Geology and Mineral Resources of South China, 27(2): 111-131 (in Chinese with English abstract).

Guo C L, Li C, Wu S C and Xu Y M. 2014. Molybdenite Re-Os isotopic dating of Xitian deposit in Hunan Province and its geological significance[J]. Rock and Mineral Analysis, 33(1): 142-152(in Chinese with English abstract).

Hanson G N, Simmons K R and Bence A E. 1975. ^{40}Ar/^{39}Ar spectrum ages for biotite, hornblende and muscovite in a contact metamorphic zone[J]. Geochimica et Cosmochimica Acta, 39(9): 1269-1278.

Heinrich C A. 1990. The chemistry of hydrothermal tin(-tungsten) ore deposition[J]. Econ. Geol., 85(3):457-481.

Hu R Z, Wei W F, Bi X W, Peng J T, Qi Y Q, Wu L Y and Chen Y W. 2012a. Molybdenite Re-Os and muscovite ^{40}Ar/ ^{39}Ar dating of the Xihuashan tungsten deposit, central Nanling district, South China[J]. Lithos, 150: 111-118.

Hu R Z and Zhou M F. 2012b. Multiple Mesozoic mineralization events in South China—an introduction to the thematic issue[J]. Mineralium Deposita, 47(6): 579-588.

Hua R M, Zhang W L, Chen P R, Zhai W and Li G L. 2013. Relationship between Caledonian granitoids and large-scale mineralization in South China[J]. Geological Journal of China Universities, 19 (1): 1-11(in Chinese with English abstract).

Hulsbosch N, Boiron M C, Dewaele S and Muchez P. 2016. Fluid fractionation of tungsten during granite-pegmatite differentiation and the metal source of peribatholitic W quartz veins: Evidence from the Karagwe-Ankole Belt (Rwanda) [J]. Geochimica et Cosmochimica Acta, 175: 299-318.

Kwak T A P. 1987. W-Sn skarn deposits and related metamorphic skarns and granitoids[M]. Amsterdam: Elsevier, 451.

Lehmann B. 1982. Metallogeny of tin: Magmatic differentiation versus geochemical heritage[J]. Econ. Geol., 77(1):50-59.

Lehmann B. 1990. Metallogeny of tin[M]. Berlin: Springer-Verlag. 211.

Li S Q, Lan X M, Deng S H, Chen S F, Wang F Y and Li C B. 2013. Metallogenic geological characteristics of Caledonian tungsten deposits in Zhenkou area of Hunan Province and ore-prospecting orientation[J]. Mineral Deposits, 32(2): 405-414(in Chinese with English abstract).

Liu X F, Yuan S D and Wu S H. 2012. Re-Os dating of the molybdenite from the Jinchuantang tin-bismuth deposit in Hunan Province and its geological significance[J]. Acta Petrologica Sinica, 28(1): 39-51(in Chinese with English abstract).

Mao J W, Xie G Q, Guo C L and Chen Y C. 2007. Large-scale tungsten-tin mineralization in Nanling region, South China: Metallogenic ages and corresponding geodynamic processes[J]. Acta Petrologica Sinica, 23(10): 2329-2338(in Chinese with English abstract).

Mao J W, Xie G Q, Guo C L, Yuan S D, Cheng Y B and Chen Y C. 2008. Spatial-temporal distribution of Mesozoic ore deposits in South China and their metallogenic settings[J]. Geological Journal of China Universities, 14(4): 510-526(in Chinese with English abstract).

Mao J W, Chen Y B and Chen M H. 2013. Major types and time-space distribution of Mesozoic ore deposits in South China and their geodynamic settings[J]. Mineralium Deposita, 48(3): 267-294.

Peng J T, Zhou M F, Hu R Z, Shen N P, Yuan S D, Bi X W, Du A D and Qu W J. 2006. Precise molybdenite Re-Os and mica Ar-Ar dating of the Mesozoic Yaogangxian tungsten deposit, Central Nanling district, South China[J]. Mineralium Deposita, 41(7): 661 -669.

Peng J T, Hu R Z, Bi X W, Dai T M , Li Z L, Li X M, Shuang Y, Yuan S D and Liu S R. 2007.40Ar/39Ar isotopic dating of tin mineralization in Furong deposit of Hunan Province and its geological significance[J]. Mineral Deposit, 26(3): 237-248(in Chinese with English abstract)

Peng J T, Hu R Z, Yuan S D, Bi X W and Shen N P. 2008. The time ranges of granitoid emplacement and related nonferrous metallic mineralization in Southern Hunan[J]. Geological Review, 54(5): 617-625 (in Chinese with English abstract).

Qiao Y S, Wang F Y, Hou M S, Lei Z H and Li C B. 2011. Geological character of Zhangjialong tungsten deposit, Hunan Province[J]. Geology and Mineral Resources of South China, 27(2): 125-131 (in Chinese with English abstract).

Qiu H N and Peng L. 1997.^{40}Ar-^{39}Ar geochronology and its applications in dating fluid inclusions[M]. Hefei: Publishing House of the University of Science and Technology of China. 54-65(in Chinese).

Shu L S, Zhou X M, Deng P and Yu X Q. 2006. Principal geological features of Nanling tectonic belt, South China[J]. Geological Review, 52(2): 251-265(in Chinese with English abstract).

Sun T. 2006. A new map showing the distribution of granites in South China and its explanatory notes[J]. Geological Bulletin of China, 25(3): 332-335(in Chinese with English abstract).

Štemprok M. 1995. A comparison of the Krušné Hory-Erzgebirge (Czech Republic-Germany) and Cornish (UK) granites and their related mineralizations[J]. Proceedings of the Ussher Society, 8: 347-356.

Taylor R G. 1979. Geology of tin deposits[M]. Amsterdam: Elsevier. 543.

Wang Y J, Fan W M , Zhao G C, Ji S and Peng T. 2007. Zircon U-Pb geochronology of gneissic rocks in the Yunkai massif and its implications on the Caledonian event in the South China Block[J]. Gondwana Research, 12(4): 404-416.

Wood S A and Samson I M. 2000. The hydrothermal geochemistry of tungsten in granitoid environments: I. relative solubilities of ferberite and scheelite as a function of *T*, *P*, pH, and *m*NaCl[J]. Econ. Geol., 95(1): 143-182.

Wu G Y, Ma T Q, Fen Y F, Yan Q R, Liu F G and Bai D Y. 2008. Geological and geochemical characteristics and genesis of the Caledonian Wanyangshan granite in the Nanling Mountains, South China[J]. Geology in China, 35(4): 608-617 (in Chinese with English abstract).

Wu J, Liang H Y, Huang W T, Wang C L, Sun W D, Sun Y L, Li J, Mo J H and Wang X Z. 2012. Indosinian isotope ages of plutons and deposits in southwestern Miaoershan-Yuechengling, northeastern Guangxi and implications on Indosinian mineralization in South China[J]. China Science Bulletin, 57(13): 1024-1035(in Chinese with English abstract).

Yang Z, Zhang W L, Wang R C, Lu J J, Xie L and Che X D. 2013.Geochronology and geochemical characteristics of metallogenetic pluton in the Youmaling tungsten mining area, northern Guangxi Province, and its geological significance[J]. Geological Journal of China Universities, (1): 159-172(in Chinese with English abstract).

Yang Z, Wang R C, Zhang W L, Chu Z Y, Chen J, Zhu J C and Zhang R Q. 2014. Skarn-type tungsten mineralization associated with the Caledonian (Silurian) Niutangjie granite, northern Guangxi, China[J]. Science China: Earth Sciences, 57(7): 1551-1566.

Yi Y S and Chen C J. 2014. Discussion on geological characteristics

and metallogenic control causes of Zhuyuanli tungsten bismuth deposit in Guidong County, Hunan Province[J]. Low Carbon World, 1: 105-107(in Chinese).

Yuan S D, Peng J T, Shen N P, Hu R Z and Dai T M. 2007. ^{40}Ar-^{39}Ar isotopic dating of the Xianghualing Sn-polymetallic orefield in southern Hunan, China and its geological implications[J]. Acta Geologica Sinca, 81(2):278-286.

Yuan S D, Peng J, Hu R, Li H, Shen N and Zhang D. 2008. A precise U-Pb age on cassiterite from the Xianghualing tin-polymetallic deposit (Hunan, South China)[J]. Mineralium Deposita, 43(4): 375-382.

Yuan S D, Peng J T, Hao S, Li H M, Geng J Z and Zhang D L. 2011. In situ LA-MC-ICP-MS and ID-TIMS U-Pb geochronology of cassiterite in the giant Furong tin deposit, Hunan Province, South China: New constraints on the timing of tin-polymetallic mineralization[J]. Ore Geology Reviews, 43(1): 235-242.

Yuan S D, Liu X F, Wang X D, Wu S H, Yuan Y B, Li X K and Wang T Z. 2012. Geological characteristics and ^{40}Ar-^{39}Ar geochronology of the Hongqiling tin deposit in southern Hunan Province[J]. Acta Petrologica Sinica, 28(12): 3787-3797(in Chinese with English abstract).

Yuan S D. 2017. Several crucial scientific issues related to the W-Sn metallogenesis in the Nanling Range and their implications for regional exploration: A review[J]. Bulletin of Mineralogy, Petrology and Geochemistry, 36(5): 736-749(in Chinese with English abstract)

Yuan S D, Williams-Jones A E, Mao J W, Zhao P L, Yan C and Zhang D L. 2018a. The origin of the Zhangjialong tungsten deposit, South China: Implications for W-Sn mineralization in large granite batholiths[J]. Econ. Geol., 113(5): 1193-1208.

Yuan S D, Mao J W, Zhao P L and Yan Y B. 2018b. Geochronology and petrogenesis of the Qibaoshan Cu polymetallic deposit, northeastern Hunan Province: Implications for the metal source and metallogenic evolution of the intracontinental Qinhang Cu-polymetallic belt, South China[J].Lithos, 302-303: 519-534.

Yuan Y B, Yuan S D, Liu X F, Mi J R, Xuan Y S and Zhao P L. 2014. Sulfur isotopic characteristics of Huangshaping granite and their geological significance in southern Hunan Province[J]. Acta Geologica Sinica, 88(12): 2437-2442(in Chinese with English abstract).

Yuan Y B, Yuan S, Mao J W, Zhao P L, Yan C, Zhao H J, Zhang D L, Shuang Y and Peng J T. 2018.Recognition of Late Jurassic W-Sn mineralization and its exploration potential on the western margin of the Caledonian Guidong granite batholith, Nanling Range, South China: Geochronological evidence from the Liuyuan Sn and Zhuyuanli W deposits[J]. Ore Geology Reviews, 93: 200-210.

Zhang D, Zhang W L, Wang R C, Chu Z Y, Gong M W and Jiang G X. 2015. Quartz-vein type tungsten mineralization associated with the Indosinian (Triassic) Gaoling granite, Miao'ershan area, northern Guangxi[J]. Geology Reviews, 61(4): 817-834 (in Chinese with English abstract).

Zhang R Q, Lu J J , Wang R C, Yang P, Zhu J C, Yao Y, Gao J F, Li C, Lei Z H, Zhang W L and Guo W M. 2015. Constraints of in situ zircon and cassiterite U-Pb, molybdenite Re-Os and muscovite ^{40}Ar-^{39}Ar ages on multiple generations of granitic magmatism and related W-Sn mineralization in the Wangxianling area, Nanling Range, South China[J]. Ore Geology Reviews, 65: 1021-1042.

Zhang Y, Chen W, Chen K L and Liu X Y. 2006. Study on the Ar-Ar age spectrum of diagenetic I/S and the mechanism of ^{39}Ar recoil loss—Examples from the clay minerals of *P-T* boundary in Changxing, Zhejiang Province[J]. Geological Review, 52(4): 556-561.

Zhang W L, Wang R C, Lei Z H, Hua R M, Zhu J C, Lu J J, Xie L, Che X D, Zhang R Q, Yao Y and Chen J. 2011. Zircon U-Pb dating confirms existence of a Caledonian scheelite-bearing aplitic vein in the Penggongmiao granite batholith, South Hunan[J]. Chinese Science Bulletin, 59(19): 1148-1154(in Chinese with English abstract).

Zhang W L, Che X D, Wang R C, Zhang R Q and Yang Z. 2014. Geochronological framework of the Penggongmiao granite batholith[J]. Acta Geologica Sinica-English Edition, 88(S2): 1041-1042.

Zhao P L, Yuan S D and Yuan Y B. 2016. Zircon LA-MC-ICP-MS U-Pb dating of the Xianglinpu granites from the Weijia tungsten deposit in southern Hunan Province and its implications for the Late Jurassic tungsten metallogenesis in the westernmost Nanling W-Sn metallogenic belt[J]. Geology in China, 43(1): 120-131(in Chinese with English abstract).

Zhao P L, Yuan S, Mao J, Santosh M and Zhang D, 2017. Zircon U-Pb and Hf-O isotopes trace the architecture of polymetallic deposits: A case study of the Jurassic ore-forming porphyries in the Qin-Hang metallogenic belt, China[J]. Lithos, 292-293: 132-145.

Zhao P L, Yuan S D, Mao J W, Yuan Y B, Zhao H J, Zhang D L and Shuang Y. 2018. Constraints on the timing and genetic link of the large-scale accumulation of proximal W-Sn-Mo-Bi and distal Pb-Zn-Ag mineralization of the world-class Dongpo orefield, Nanling Range, South China[J]. Ore Geology Reviews, 95: 1140-1160.

附中文参考文献

陈文,张彦,金贵善,张岳桥. 2006. 青藏高原东南缘晚新生代幕式抬升作用的Ar-Ar热年代学证据[J]. 岩石学报, 22(4): 867-872.

陈文迪,张文兰,王汝成,储著银,肖荣,张迪,车旭东. 2016. 桂北苗儿山-越城岭地区独石岭钨(铜)矿床研究:对复式岩体多时代差异性成矿的启示[J]. 中国科学:地球科学, 46(12): 52-75.

蔡杨,马东升,陆建军,黄卉,章荣清,屈文俊. 2012. 湖南邓阜仙钨矿辉钼矿铼-锇同位素定年及硫同位素地球化学研究[J]. 岩石学报, 28(12): 3798-3808.

郭爱民. 2011. 湖南资兴张家垄钨矿床地质特征及找矿前景分析[J]. 华南地质与矿产, 27(2): 111-117.

郭春丽,李超,伍式崇,许以明. 2014. 湘东南锡田辉钼矿 Re-Os 同位素定年及其地质意义[J]. 岩矿测试, 33(1): 142-152.

华仁民,张文兰,陈培荣,翟伟,李光来. 2013. 初论华南加里东花岗岩与大规模成矿作用的关系[J]. 高校地质学报, 19(1): 1-11.

李时谦,蓝晓明,邓松华,陈尚峰,王方有,黎传标. 2013. 湖南圳口地区加里东期钨矿田成矿地质特征及找矿方向[J]. 矿床地质, 32(2): 405-414.

刘晓菲,袁顺达,吴胜华. 2012. 湖南金船塘锡铋矿床辉钼矿 Re-Os 同位素测年及其地质意义[J]. 岩石学报, 28(1): 39-51.

毛景文, 谢桂青, 郭春丽, 陈毓川. 2007. 南岭地区大规模钨锡多金属成矿作用: 成矿时限及地球动力学背景[J]. 岩石学报, 23(10): 2329-2338.

毛景文,谢桂青,郭春丽,袁顺达,程彦博,陈毓川. 2008. 华南地区中生代主要金属矿床时空分布规律和成矿环境[J]. 高校地质学报, 14(4): 510-526.

彭建堂,胡瑞忠,毕献武,戴橦谟,李兆丽,李晓敏,双燕,袁顺达, 刘世荣. 2007. 湖南芙蓉锡矿床 $^{40}Ar/^{39}Ar$同位素年龄及地质意义[J]. 矿床地质, 26(3): 237-248.

彭建堂,胡瑞忠,袁顺达,毕献武,沈能平. 2008. 湘南中生代花岗质岩石成岩成矿的时限[J]. 地质论评, 54(5): 617-625.

乔玉生,王方有,侯茂松,雷泽恒,黎传标. 2011. 湖南张家垄矿区钨矿地质特征[J]. 华南地质与矿产, 27(2): 125-131.

邱华宁,彭良. 1997. ^{40}Ar-^{39}Ar年代学与流体包裹体定年[M]. 合肥:中国科学技术大学出版社. 54-65.

舒良树,周新民,邓平,余心起. 2006. 南岭构造带的基本地质特征[J]. 地质论评, 52(2): 251-265.

孙涛. 2006. 新编华南花岗岩分布图及其说明[J]. 地质通报, 25(3): 332-335.

伍光英,马铁球,冯艳芳,闫全人,刘富国,柏道远. 2008. 南岭万洋山加里东期花岗岩地质地球化学特征及其成因[J]. 中国地质, 35(4): 608-617.

伍静,梁华英,黄文婷,王春龙,孙卫东,孙亚莉,李晶,莫济海,王秀璋. 2012. 桂东北苗儿山-越城岭南西部岩体和矿床同位素年龄及华南印支期成矿分析[J]. 科学通报, 57(13): 1126-1136.

杨振,张文兰,王汝成,陆建军,谢磊,车旭东. 2013. 桂北油麻岭钨矿区成矿岩体的年代学、地球化学及其地质意义[J]. 高校地质学报, 1: 159-172.

杨振,王汝成,张文兰,储著银,陈骏,朱金初,章荣清. 2014. 桂北牛塘界加里东期花岗岩及其矽卡岩型钨矿成矿作用研究[J]. 中国科学:地球科学, 44(7): 1357-1373.

易元顺,陈长江. 2014. 湖南省桂东县竹园里钨铋矿床地质特征与成矿控制因的的探讨[J]. 低碳世界, 1: 105-107.

袁顺达,刘晓菲,王旭东,吴胜华,原垭斌,李雪凯,王铁柱. 2012. 湘南红旗岭锡多金属矿床地质特征及 Ar-Ar 同位素年代学研究[J]. 岩石学报, 28(12): 3787-3797.

袁顺达.2017.南岭钨锡成矿作用几个关键科学问题及其对区域找矿勘查的启示[J]. 矿物岩石地球化学通报, 36(5):736-749

原垭斌,袁顺达,刘晓菲,弥佳茹,轩一撒,赵盼捞. 2014. 湘南黄沙坪矿区花岗岩的硫同位素特征及其地质意义[J]. 地质学报, 88(12): 2437-2442.

张迪,张文兰,王汝成,储著银,龚名文,蒋桂新. 2015. 桂北苗儿山地区高岭印支期花岗岩及石英脉型钨成矿作用[J]. 地质论评, 61(4): 817-834.

张彦,陈文,陈克龙,刘新宇. 2006. 成岩混层(I/S)Ar-Ar 年龄谱型及 ^{39}Ar 核反冲丢失机理研究—以浙江长兴地区 *P-T* 界线粘土岩为例[J]. 地质论评, 52(4): 556-561.

张文兰,王汝成,雷泽恒,华仁民,朱金初,陆建军,谢磊,车旭东, 章荣清,姚远,陈骏. 2011. 湘南彭公庙加里东期含白钨矿细晶岩脉的发现[J]. 科学通报, 56(18): 1448-1454.

赵盼捞,袁顺达,原亚斌. 2016. 湘南魏家钨矿区祥林铺岩体锆石 LA-MC-ICP-MS U-Pb 测年——对南岭西端晚侏罗世钨成岩成矿作用的指示[J]. 中国地质, 43(1): 120-131.